LHC limits on gluinos and squarks in the minimal Dirac gaugino model.

Humberto Reyes-González
LPSC, Grenoble.

Work in collaboration with:
G. Chalons, M. Goosell, S. Kraml and S. Williamson

ALPS 2019, Obergurgl, Austria, 26 April 2019

Introduction.

- In the MSSM gauginos (superpartners of the gauge bosons) are majorana particles described by Weyl fermions.
- To have Dirac gaugino masses, new chiral supermultiplets are added. Suggesting an enriched phenomenology.

Some nice features of Dirac gaugino models:

- Dirac gauginos were originally proposed by Fayet (1978) to allow massive gluinos.
- Increased naturalness: supersoft masses do not lead to large correction of the stop mass.
- Enhanced tree level Higgs mass.

Motivation:

- Most of SUSY searches at the LHC are optimised for the MSSM (Minimal SuperSymmetric Model)
- A difference in limits from LHC results is expected as compared to the MSSM when observing gluino and squark production.

We'll set limits on the gluinos and squarks of a MDGSSM, by re-interpreting LHC results.

Particle content of the MDGSSM.

Names		Spin 0	Spin 1/2	Spin 1	$SU(3),\ SU(2),\ U(1)_Y$
Quarks	$\mathbf{Q}$	$\tilde{Q} = (\tilde{u}_L\,, \tilde{d}_L)$	$(u_L\,, d_L)$		$(\mathbf{3},\ \mathbf{2},\ 1/6)$
	$\mathbf{u^c}$	$\tilde{u}_L^c$	u_L^c		$(\bar{\mathbf{3}},\ \mathbf{1},\ \text{-}2/3)$
($\times$3 families)	$\mathbf{d^c}$	$\tilde{d}_L^c$	u_L^c		$(\bar{\mathbf{3}},\ \mathbf{1},\ 1/3)$
Leptons	$\mathbf{L}$	$(\tilde{\nu}_{eL},\tilde{e}_L)$	$(\nu_{eL}\,, e_L)$		$(\mathbf{1},\ \mathbf{2},\ \text{-}1/2)$
($\times$3 families)	$\mathbf{e^c}$	$\tilde{e}_L^c$	e_L^c		$(\mathbf{1},\ \mathbf{1},\ 1)$
Higgs	$\mathbf{H_u}$	$(H_u^+\,, H_u^0)$	$(\tilde{H}_u^+\,, \tilde{H}_u^0)$		$(\mathbf{1},\ \mathbf{2},\ 1/2)$
	$\mathbf{H_d}$	$(H_d^0\,, H_d^-)$	$(\tilde{H}_d^0\,, \tilde{H}_d^-)$		$(\mathbf{1},\ \mathbf{2},\ \text{-}1/2)$
Gluons	$\mathbf{W}_{3\alpha}$		$\tilde{g}_\alpha$	g	$(\mathbf{8},\ \mathbf{1},\ 0)$
W	$\mathbf{W}_{2\alpha}$		$\tilde{W}^\pm,\ \tilde{W}^0$	$W^\pm,\ W^0$	$(\mathbf{1},\ \mathbf{3},\ 0)$
B	$\mathbf{W}_{1\alpha}$		$\tilde{B}$	B	$(\mathbf{1},\ \mathbf{1},\ 0)$
DG-octet	$\mathbf{O_g}$	O_g	$\tilde{g}'$		$(\mathbf{8},\ \mathbf{1},\ 0)$
DG-triplet	$\mathbf{T}$	$\{T^0,\ T^\pm\}$	$\{\tilde{W}'^\pm,\ \tilde{W}'^0\}$		$(\mathbf{1},\mathbf{3},\ 0)$
DG-singlet	$\mathbf{S}$	S	$\tilde{B}'$		$(\mathbf{1},\ \mathbf{1},\ 0)$

Chiral and gauge multiplet fields in the model

MSSM

MDGSSM

Electroweakino sector.

New Higgs superpotential couplings between the singlet and triplet DG-adjoint fermions and the Higgs higgsino fields:

$$W_{\text{Higgs}} = \mu\, \mathbf{H_u} \cdot \mathbf{H_d} + \lambda_S \mathbf{S}\, \mathbf{H_u} \cdot \mathbf{H_d} + 2\lambda_T\, \mathbf{H_d} \cdot \mathbf{T} \mathbf{H_u}.$$

In the MDGGSM, gauginos are purely Dirac, i.e. $M_1 = M'_1 = M_2 = M'_2 = 0$. m_{1D} and m_{2D} are the bino and wino Dirac masses.

$$\mathcal{L} \supset \frac{1}{2} M_i \lambda_i \lambda_i + h.c.$$

$$\mathcal{L} \supset -m_{iD} \chi_i \lambda_i + h.c.$$

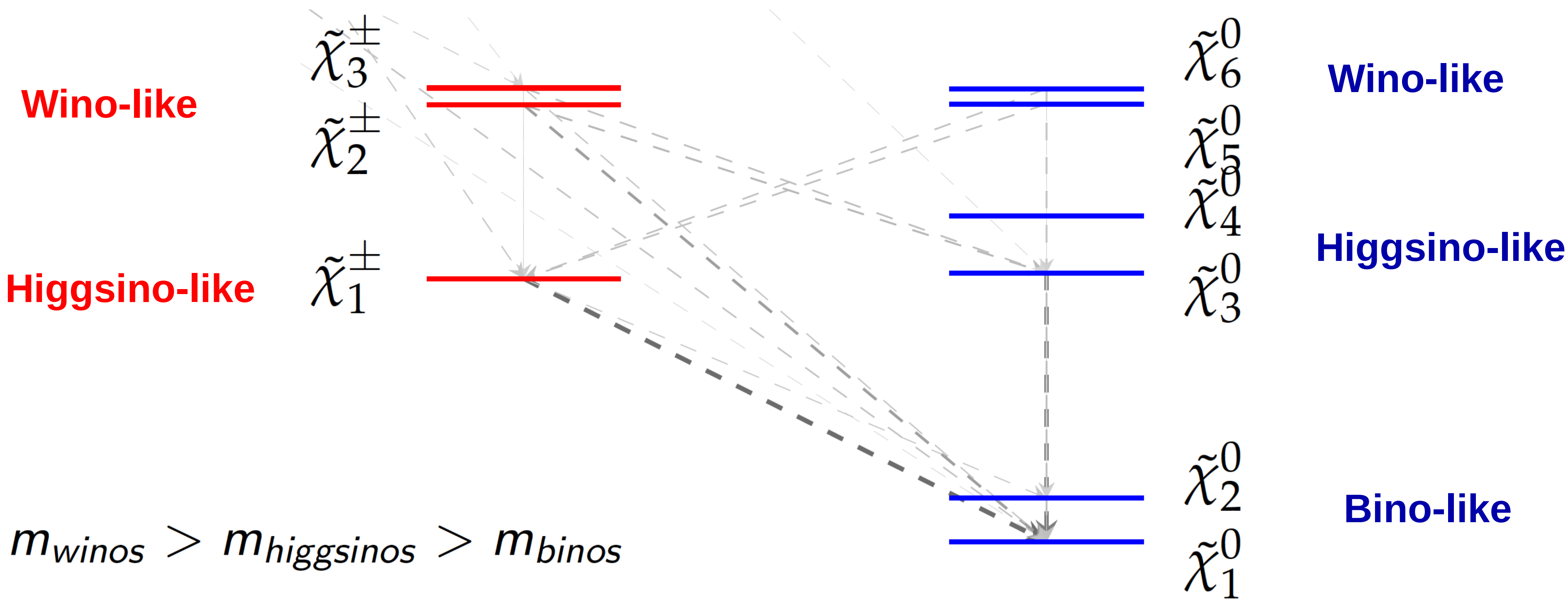

$$m_{winos} > m_{higgsinos} > m_{binos}$$

Gluino and squark production (comparison with MSSM).

- **Squark pair production.** t-channel exchange of the Dirac gluino forbids final states with squarks of the same helicity, reducing squark production cross section. ⟶
- **Gluino pair production.** Cross section enhanced because there are more gluino-degrees of freedom.
- **Gluino-squark production.** This is identical to the Majorana case.

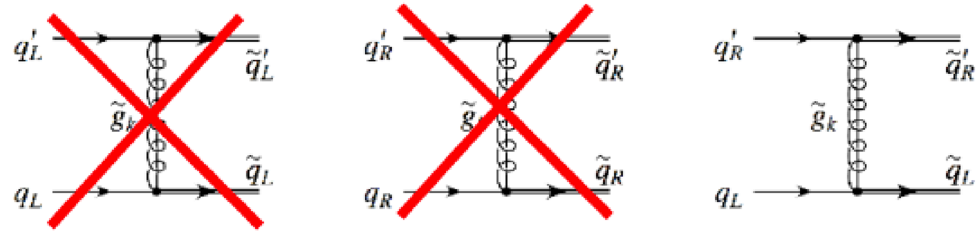

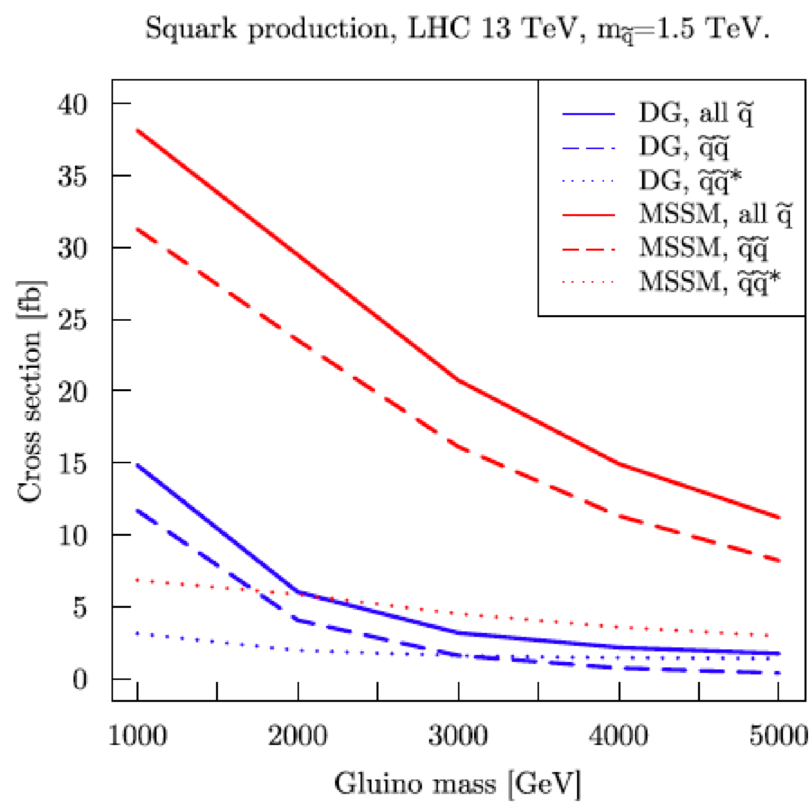

arXiv:1111.4322

Lifetime and mass splitting of binos: motivation of benchmark choices.

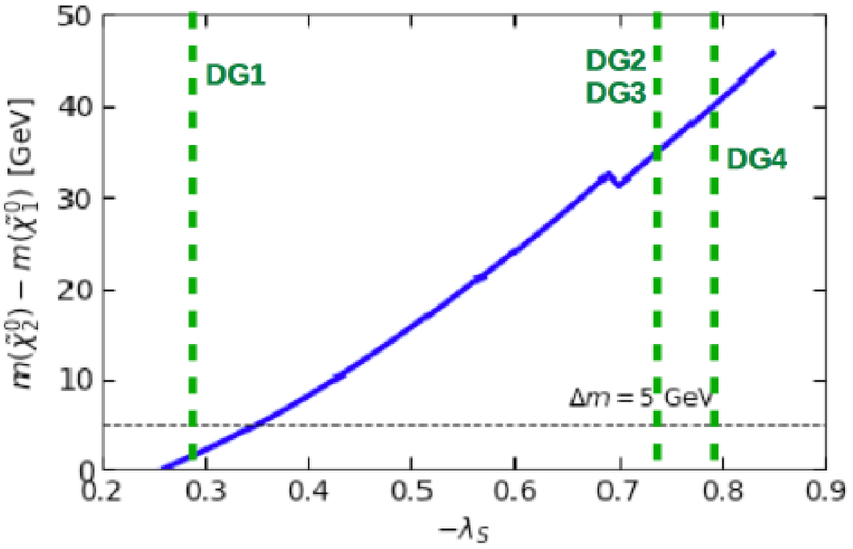

Mass splitting between $\tilde{\chi}_{1,2}^0$.

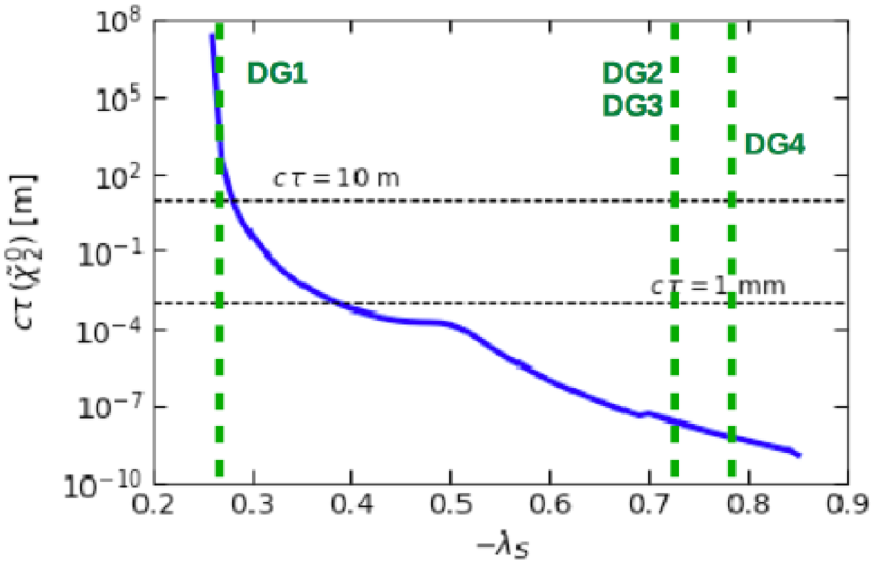

The lifetime of $\tilde{\chi}_2^0$.

Constraints for four benchmark scenarios will be shown:

- One with small $\tilde{\chi}_{1,2}^0$ mass spliting/long $\tilde{\chi}_2^0$ lifetime: DG1 where λ_S=-0.27 .
- Three with a large $\tilde{\chi}_{1,2}^0$ mass spliting/short $\tilde{\chi}_2^0$ lifetime: DG2,DG3 with λ_S =-0.74 and DG4 with λ_S =-0.79.

Benchmark scenarios.

Parameters				
	DG1	DG2	DG3	DG4
m_{1D}	200	200	200	200
m_{2D}	500	500	500	1175
μ	400	400	400	400
$\tan\beta$	2	2	2	2
$-\lambda_S$	0.27	0.74	0.74	0.79
$\sqrt{2}\,\lambda_T$	0.14	0.14	0.14	-0.26
$m^2_{\tilde{Q}_3}$	1.25e7	6.5e6	2.26e6	8.26e6
$m^2_{\tilde{Q}_1}$	6.25e6	6.25e6	6.25e6	6.25e6
m_{3D}	1750	1750	1750	1750

Masses				
	DG1	DG2	DG3	DG4
$\tilde{\chi}^0_1$	201.35	182.1	181.8	182.4
$\tilde{\chi}^0_2$	201.72	218.0	216.6	213.2
$\tilde{\chi}^0_3$	403	400	396	408
$\tilde{\chi}^0_4$	419	445	441	437
$\tilde{\chi}^0_5$	537	536	535	1226
$\tilde{\chi}^0_6$	548	548	546	1227
$\tilde{\chi}^\pm_1$	400	395	391	398
$\tilde{\chi}^\pm_2$	536	536	534	1224
$\tilde{\chi}^\pm_3$	549	548	547	1229
$\tilde{t}_1$	3604	2607	1590	2894
$\tilde{t}_2$	3613	2637	1613	2927
h_1	124.0	125.0	125.3	125.2

Small bino mass splitting.
Large bino mass splitting.
Light winos.
Heavy winos.

We scanned over the gluino and squark mass spectrum.

Constraining with two approaches: SMS and Recasting.

Simplified Model Spectrum results

- SModelS: Based on the general procedure to decompose BSM collider signatures presenting a Z2 symmetry into Simplified Model Spectrum (SMS) topologies. (arXiv:1811.10624)

Full recasting.

- This approach involves full chain event simulation, performed with a Madgraph-Pythia8-Delphes pipeline.
- Recasting and analysis performed with MadAnalysis

Results from SModelS.

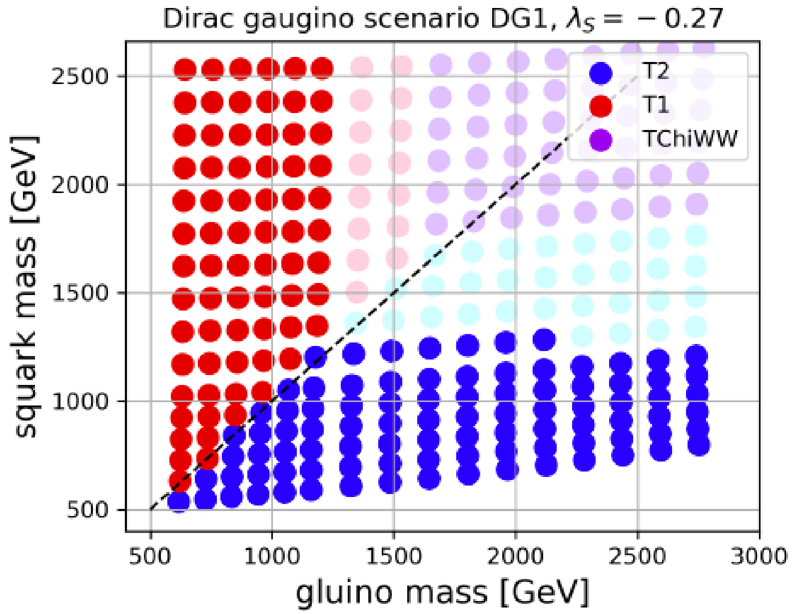

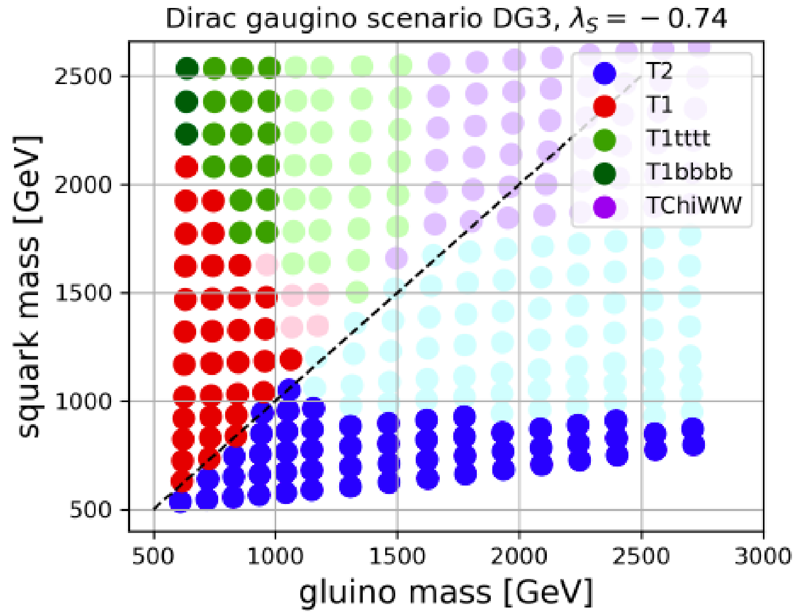

Gluino vs squark masses map of the SModelS limits. Hard coloured points means exclusion.

T1: $pp \to \tilde{g}\tilde{g},\ \tilde{g} \to q\bar{q}\tilde{\chi}_1^0$; T1tttt: $pp \to \tilde{g}\tilde{g},\ t\bar{t}\tilde{\chi}_1^0$; T2: $pp \to \tilde{q}\tilde{q}^{(*)}, \tilde{q} \to q\tilde{\chi}_1^0$; TChiWW: $pp \to \tilde{\chi}_i^{\pm}\tilde{\chi}_i^{\pm},\ \tilde{\chi}_i^{\pm} \to W^{\pm}\tilde{\chi}_1^0$

Due to the complexity of the model, constraints from SMS are weaker. E.g. The effective cross section from the T1 topology above is roughly 1% of the total.

ATLAS SUSY 2016-07: The recasted analysis.

Search for squarks and gluinos in final states with jets and missing transverse momentum using 36 fb^{-1} of $\sqrt{s}$ =13 TeV pp collision data with the ATLAS detector

ATLAS analyses, 13 TeV

Analysis	Short Description	Implemented by	Code	Validation note	Version
ATLAS-SUSY-2015-06	Multijet + missing transverse momentum	S. Banerjee, B. Fuks, B. Zaldivar	Inspire	PDF	v1.3/Delphes3
ATLAS-SUSY-2016-07	Multijet + missing transverse momentum (36.1 fb-1)	G. Chalons, H. Reyes-Gonzalez	Inspire	PDF Pythia files	v1.7/Delphes3
ATLAS-EXOT-2015-03	Monojet (3.2 fb-1)	D. Sengupta	Inspire	PDF	v1.3/Delphes3
ATLAS-EXOT-2016-25	Mono-Higgs (36.1 fb-1)	S. Jeon, Y. Kang, G. Lee, C. Yu	Inspire	PDF	v1.6/Delphes3
ATLAS-EXOT-2016-27	Monojet (36.2 fb-1)	D. Sengupta	Inspire	PDF	v1.6/Delphes3
ATLAS-EXOT-2016-32	Monophoton (36.1 fb-1)	S. Baek, T.H. Jung	Inspire	PDF	v1.6/Delphes3
ATLAS-CONF-2016-086	b-pair + missing transverse momentum	B. Fuks & M. Zumbihl	Inspire	PDF	v1.6/Delphes3

http://madanalysis.irmp.ucl.ac.be/wiki/PublicAnalysisDatabase

Results from Recasting : DG1-3 vs MSSM1 (light winos).

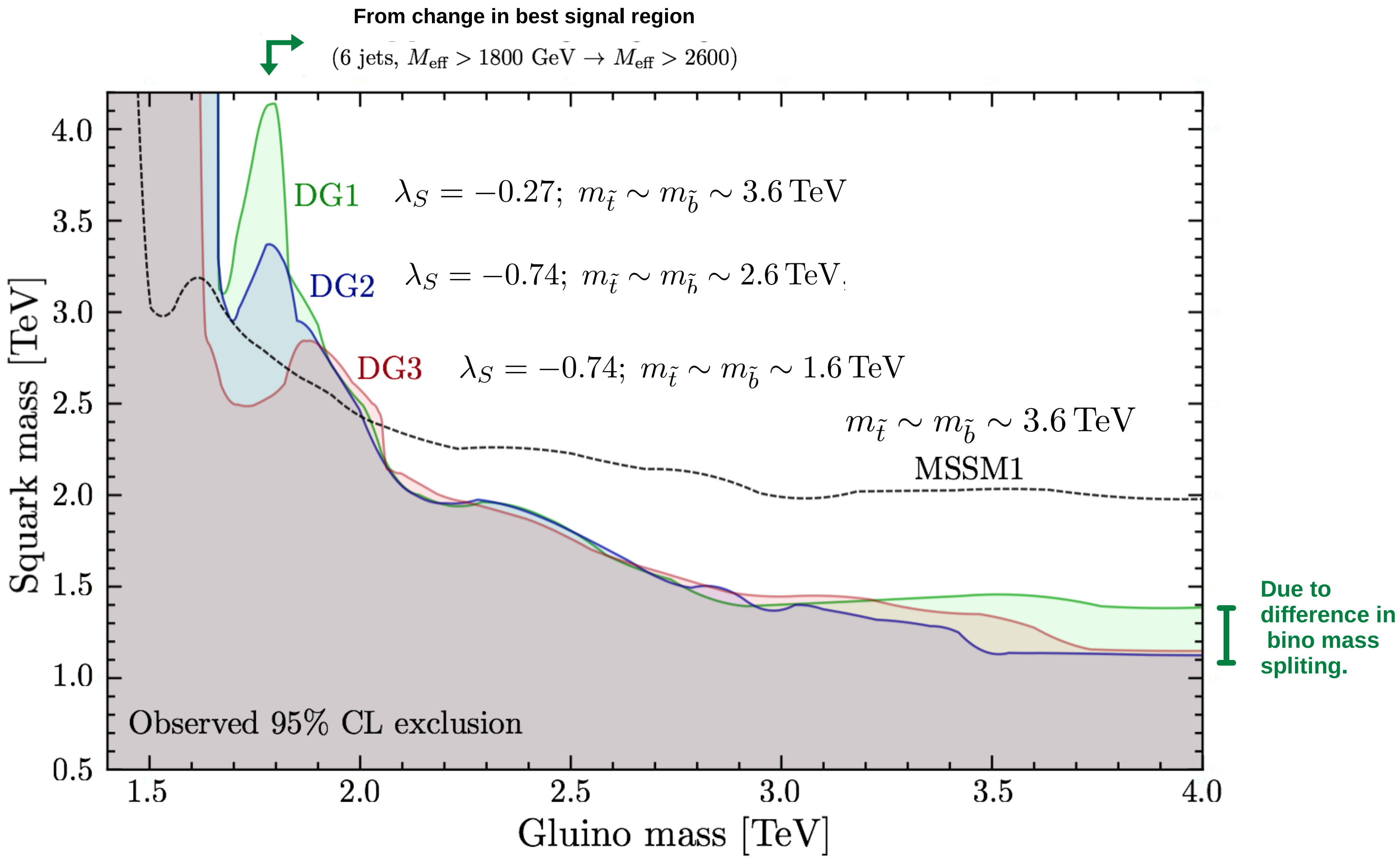

MSSM1 and DG1 are equivalent.

Results from Recasting : DG4 vs MSSM4 (heavy winos).

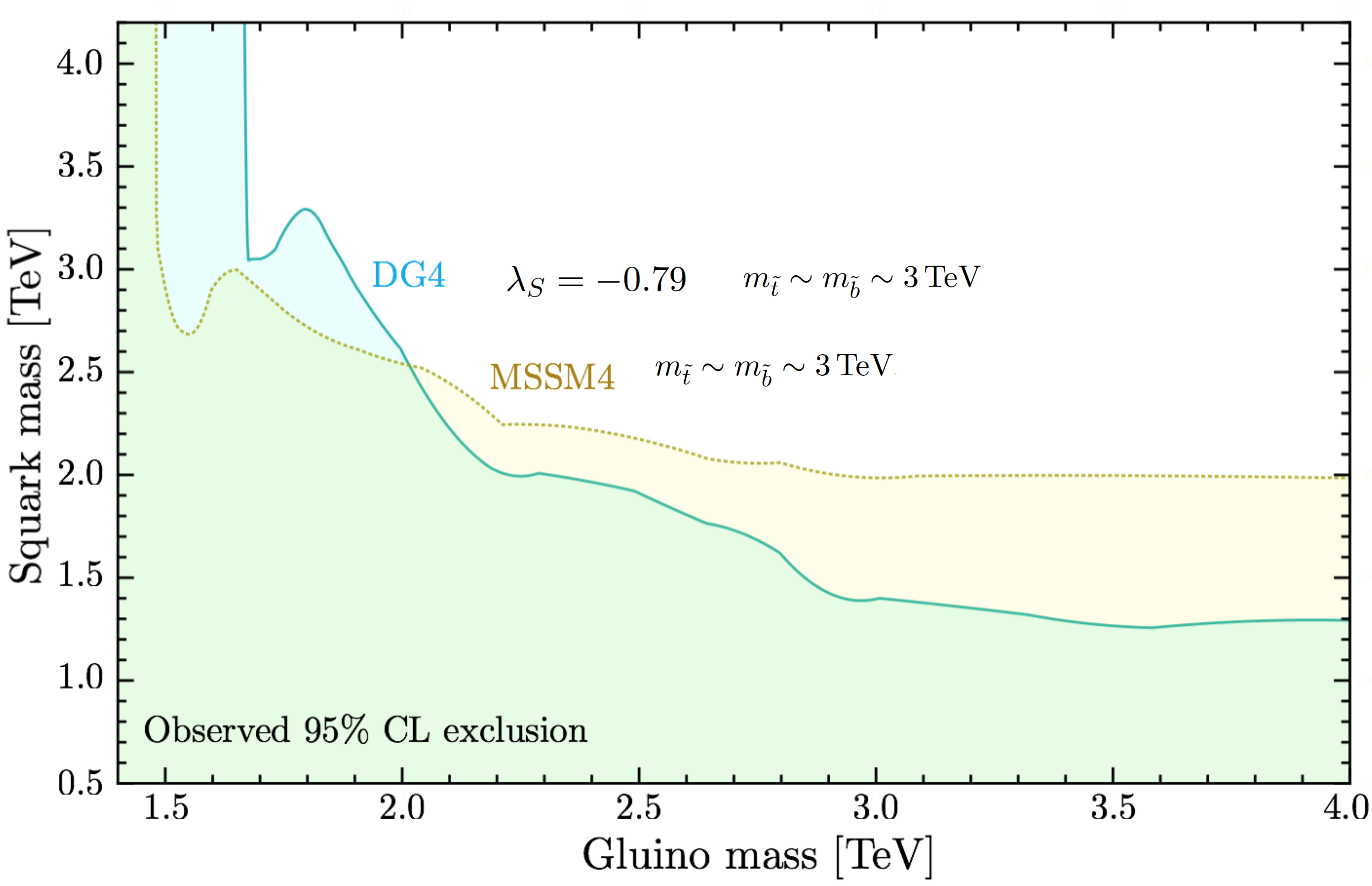

Conclusions.

- Bounds on squarks and gluinos were found for 4 benchmark scenaros of the MDGSSM and compared with equivalent MSSM scenarios.
- Results were as expected from the differences between MDGSSM and MSSM regarding gluino and squark production.
- We observed relaxed contstraints in the scenarios with large bino mass-splitting due to extra steps in the decay chain.

Outlook.

- Study limits on the electroweak sector.
- Look for scenarios where the LSP (dark matter candidate) has a relic density equal or below the one measured by Planck.
- Study scenarios with small bino mass splitting in the light of Long Lived Particle searches.

Thank you!

CLs for DG4 with k-factors

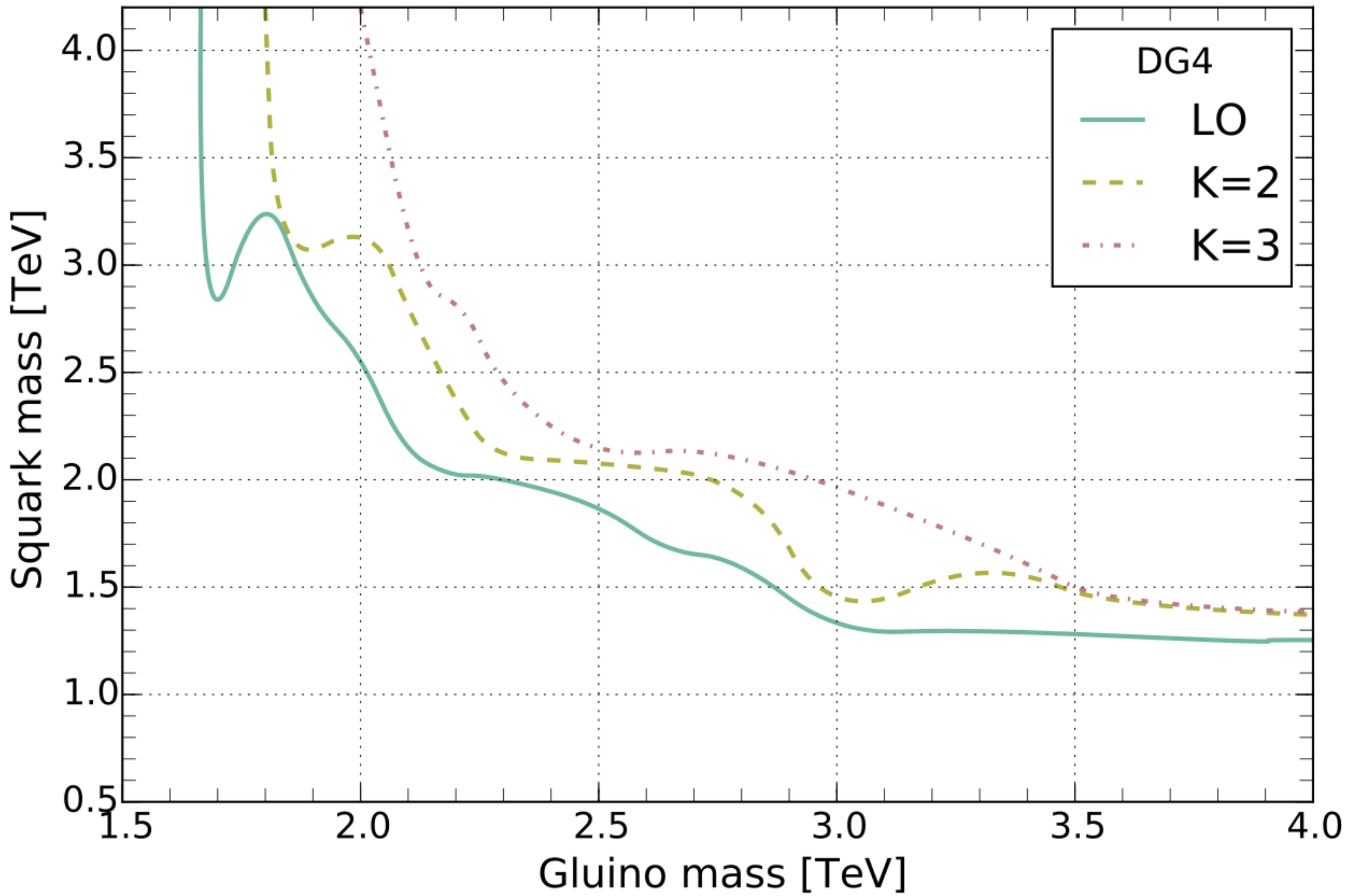

Electroweakino mass matrices in the MDGSSM.

$$\mathcal{M}_N = \begin{pmatrix} 0 & m_{1D} & 0 & 0 & \frac{\sqrt{2}\lambda_S}{g'} m_Z s_W s_\beta & \frac{\sqrt{2}\lambda_S}{g'} m_Z s_W c_\beta \\ m_{1D} & 0 & 0 & 0 & -m_Z s_W c_\beta & m_Z s_W s_\beta \\ 0 & 0 & 0 & m_{2D} & -\frac{\sqrt{2}\lambda_T}{g} m_Z c_W s_\beta & -\frac{\sqrt{2}\lambda_T}{g} m_Z c_W c_\beta \\ 0 & 0 & m_{2D} & 0 & m_Z c_W c_\beta & -m_Z c_W s_\beta \\ \frac{\sqrt{2}\lambda_S}{g'} m_Z s_W s_\beta & -m_Z s_W c_\beta & -\frac{\sqrt{2}\lambda_T}{g} m_Z c_W s_\beta & m_Z c_W c_\beta & 0 & -\mu \\ \frac{\sqrt{2}\lambda_S}{g'} m_Z s_W c_\beta & m_Z s_W s_\beta & -\frac{\sqrt{2}\lambda_T}{g} m_Z c_W c_\beta & -m_Z c_W s_\beta & -\mu & 0 \end{pmatrix}$$

$$\mathcal{M}_C = \begin{pmatrix} 0 & m_{2D} & \frac{2\lambda_T}{g} m_W c_\beta \\ m_{2D} & 0 & \sqrt{2} m_W s_\beta \\ -\frac{2\lambda_T}{g} m_W s_\beta & \sqrt{2} m_W c_\beta & \mu \end{pmatrix}$$

Binos, Winos, Higgsinos.

Best signal region evolution.

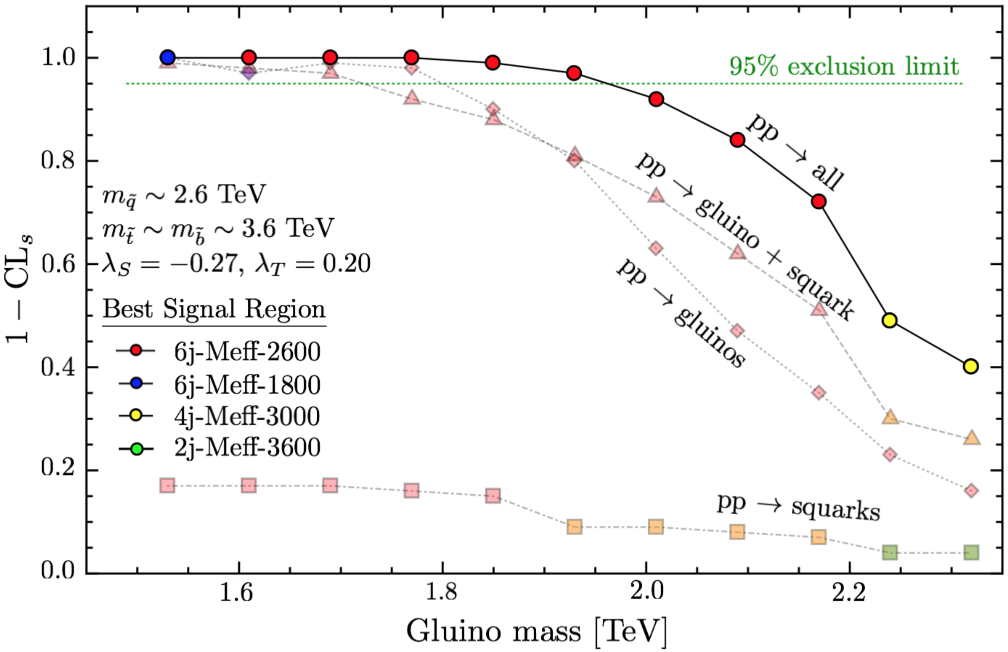

DG1

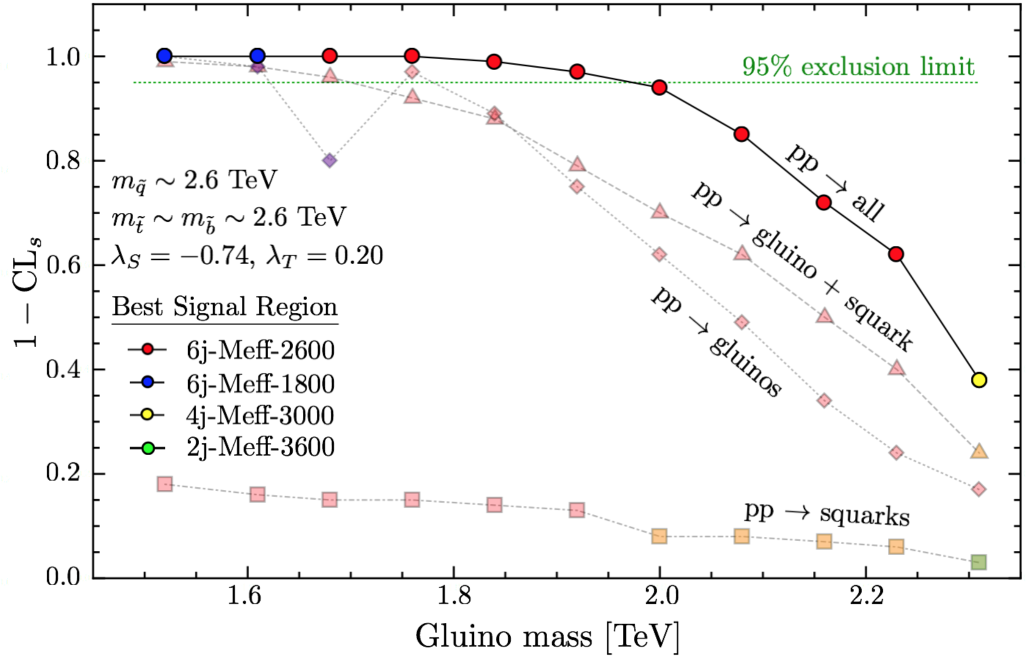

DG2

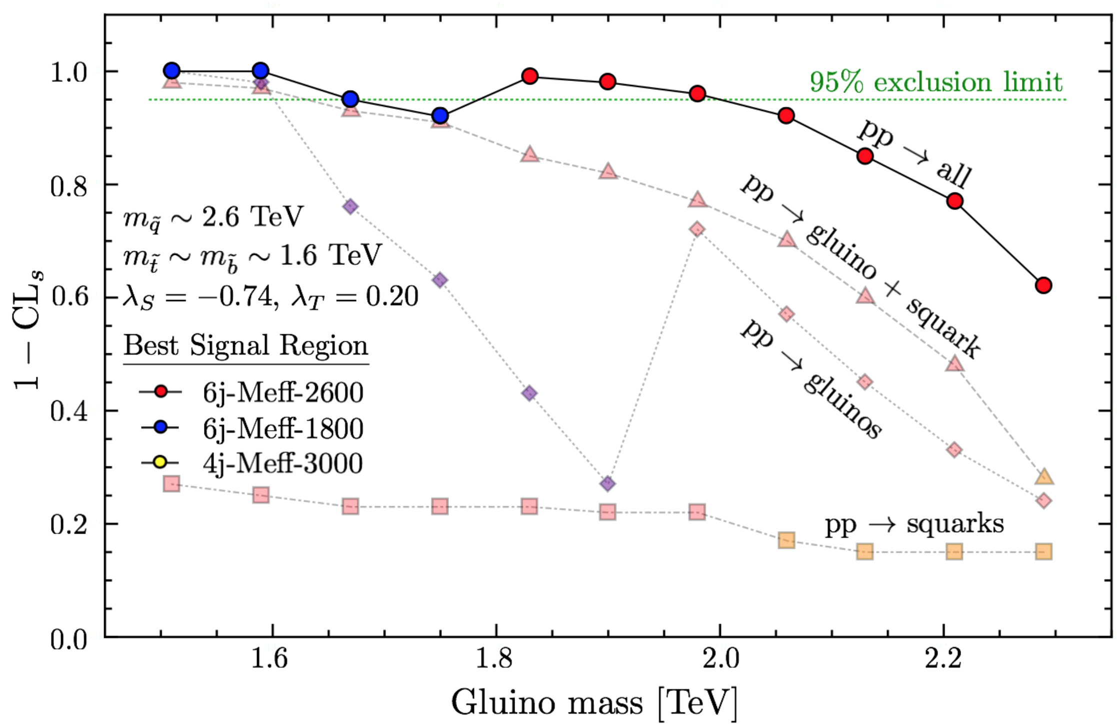

DG3